Nonsense mutations can also increase mRNA levels

Precious O. Owuamalam [a], Md. Nazmul Hossain [a], and Saverio Brogna [a,*]

[a] School of Biosciences and Birmingham Centre for Genome Biology (BCGB), University of Birmingham, Edgbaston, B15 2TT, United Kingdom

* Correspondence: s.brogna@bham.ac.uk

Abstract

Nonsense mutations are frequently associated with reduced mRNA levels due to premature translation termination triggering nonsense-mediated mRNA decay (NMD). We introduced premature termination codons (PTCs) at 15 different positions within the coding region of a GFP reporter gene in *Schizosaccharomyces pombe*. Mutations located in the first third of the coding region typically led to decreased mRNA levels, whilst those occurring further downstream caused either no change or only minor reductions, consistent with current splicing-independent NMD models. However, PTCs located closer to the normal stop codon unexpectedly resulted in increased mRNA levels compared to the PTC-less control transcript. Analysis of intron-containing versions of these constructs confirmed that splicing enhances the impact of a nonsense mutation on mRNA levels. As expected, deletion of *UPF1* in wild-type cells increased the levels of transcripts normally reduced by NMD. Interestingly, it also further increased the levels of transcripts that were already elevated compared to the PTC-less control in the wild-type background. The greater abundance of these mRNAs does not appear to be due to increased mRNA stability. Notably, a PTC located near the end of the coding sequence not only resulted in increased mRNA levels, but also in the production of a truncated, yet functional, GFP protein. These observations challenges current key assumptions about the significance of NMD.

Keywords: Nonsense-mediated mRNA decay, UPF1, Splicing, mRNA surveillance, GFP.

Introduction

Nonsense mutations result in reduced mRNA levels. This phenomenon has been observed in all investigated organisms, from bacteria to mammals (1). The reduction in mRNA levels is attributed to a specialised mRNA decay pathway, which detects and rapidly destroys aberrant mRNAs characterised by the presence of a stop codon in abnormal locations, thereby protecting cells against the production of potentially deleterious truncated proteins (1). This nonsense-mediated mRNA decay (NMD) pathway relies on conserved protein-transacting factors across eukaryotes. The most conserved factors include UPF1, UPF2, and UPF3, which recognize and eliminate the aberrant transcripts (2-4).

NMD is linked to pre-mRNA splicing. In mammalian systems, the deposition of the exon-junction complex of proteins upstream of a splice junction, after splicing in the nucleus (5, 6), is thought to serve as the connection. Additionally, in mammals, over 90% of the genes contain introns (7), and apart from a few instances, genes without introns are usually immune to NMD (8-10). However, in fission yeast, *Schizosaccharomyces pombe*, introns are not essential for NMD (11, 12). Here, early nonsense mutations are subject to NMD but not later PTC-containing transcripts. However, in the presence of introns, the sensitivity of NMD depends on the distance between the mutation and the intron (11). The farther a PTC is from an intron, the less likely it is to be subject to NMD, which would not be the case for early PTCs, because, regardless of intron presence, they are still subject to NMD.

In *S. pombe*, the core components of the exon junction complex (EJC), Y14, Mago, and eIF4AIII (excluding MLN51), are conserved. The absence of an MLN51 homolog, which stabilizes the EJC in mammalian cells(13) suggests that a stable EJC is likely absent in *S. pombe*. Previously, we showed that deleting the EJC core components did not suppress NMD in *S. pombe* (11). While splicing might enhance translation in yeast (16, 17), in our previous study, we observed the opposite. Splicing decreased the translation of the reporters, implying that the increased severity of NMD observed in the presence of an intron is possibly not due to the enhanced translation of the reporters (11). That splicing enhanced NMD regardless of PTC position cannot be explained by the EJC in *S. pombe*. Based on that observation, in this current study we aimed to understand the mechanism linking splicing to NMD. Unexpectedly, we found that a nonsense mutation can also lead to increased mRNA levels. When NMD was observed in the 1970s (14), it was thought to be a passive mechanism that destroys aberrant mRNAs because they are not shielded by the ribosome (15). That we see that nonsense mutations can increase mRNA levels does not fit the mRNA surveillance hypothesis. If an mRNA with a nonsense mutation can potentially lead to a truncated protein, which is toxic, then a good mRNA surveillance mechanism would destroy that transcript. We find that a nonsense mutation near the end of the coding region does not do this; instead, it increases rather than decreases mRNA levels. The truncated protein is more functional since we make more of the RNA, and in one case observe increased reporter protein expression.

Results

PTC position on the coding sequence is a key determinant of NMD sensitivity

In order to extend our previous analysis on the effect of nonsense mutations on mRNA levels, we generated additional constructs at GFP codon positions 1, 40, 53, 70, 88, 108, 112, 126, 141, 161, 185, 210, and 231, totalling 15 PTCs, including PTC6 and PTC27 from our previous study (Figure 1A) (11). We integrated these constructs (where GFP is under the control of the *nmt41* promoter and *adh1* terminator) into the *leu1* chromosomal locus in a wild-type (WT) *S. pombe* strain as previously described (11) to minimize cell-to-cell variation that can be caused by differences in plasmid copy number. We observed that mutations in positions 1-88 cause significant changes in mRNA levels (Figure 1B). However, with PTCs located further downstream from PTC108 (with the exception of PTC126), there was no change in mRNA levels. Surprisingly, 3 of the PTC mutations (PTCs 141, 185, and 231) led to increased mRNA levels. We have annotated as Region 1, the PTCs located early in the coding region, which caused reduced mRNA levels (PTC1-88), and Region 2 (PTC108-231), the mutations located further downstream, which cause no change in mRNA levels, or surprisingly increased mRNA levels (Figure 1A, C). When we compared the mean fold changes between the two regions, we observed a significant difference in their mean fold changes, further reinforcing the difference in NMD sensitivity between the two regions (Figure 1C).

To examine whether the observed mRNA reduction depends on *UPF1*, we selected two mutations from the two regions, PTC6 (Region 1) and PTC141 (Region 2). Deletion of *UPF1* increased PTC6 mRNA levels, but surprisingly further increased PTC141 mRNA levels, which were already significantly higher than in PTC-less GFP (WT-GFP) (Figure 1D). We then examined the changes in RNA stability. PTC6 had lower mRNA stability than WT-GFP, and deletion of *UPF1* partially increased its stability (Figure 1E). WT-GFP and *Δupf1*-GFP were quite stable, while GFP PTC6 and *Δupf1*-GFP-PTC6 had approximate half-lives of around 14 minutes and 40 minutes, respectively. While the increase in GFP-PTC6 mRNA levels (Figure 1D) could be explained by increased RNA stability, that of PTC 141 cannot. While we didn't test RNA stability changes between WT-GFP and GFP-PTC141, we didn't observe any significant changes in the stability of GFP-PTC141 (which produced more mRNA than the WT-GFP) compared to WT-GFP (Figure 1F).

One of the criteria for selecting the PTC positions (shown in Figure 1A) was the presence of an ATG codon downstream. This is to determine if translation can be re-initiated at a downstream ATG, potentially suppressing the PTC-induced NMD. The next methionine codon after the first ATG is located at codon position 79, nine codons away from PTC70 (Supplementary Figure 1A). Comparing PTC70 transcript levels to PTC53 suggests that translation re-initiation might be occurring in this case. However, PTC70 showed similar transcript levels to other early PTCs, negating this possibility. Additional methionine codons are located at positions 89, 154, 219, and 234. When comparing transcript levels of PTCs upstream of these methionine codons with those further upstream or downstream, there is no correlation, indicating that a putative translation re-initiation mechanism suppresses NMD. Similar transcript levels were observed even without a downstream ATG codon. Next, we examined how the nonsense mutations affected GFP fluorescence. While we did not observe any detectable GFP fluorescence with the PTC reporters, GFP fluorescence was observed with PTC231 (Supplementary Figure 1B). In fact, the fluorescence levels achieved were twice as high as the WT-GFP fluorescence (Supplementary Figure 1C). Altogether, our data shows that a PTC can cause an increase as well as a decrease in mRNA levels, independent of transcript stability.

Splicing alters the effect of nonsense mutations on mRNA levels

Previously, we showed that splicing enhances NMD in *S. pombe* (11). To further explore how PTC mutations affect NMD depending on the intron's position, we created intron-containing versions of the reporters from Figure 1A (Figure 2A) and integrated the pDUAL-GFPivs-PTC-containing reporters into the *leu1* locus in WT *S. pombe*. We observed that nonsense mutations located throughout the GFP coding region, regardless of if they are located upstream (Region 1) or further downstream (Region 2), result in a reduction in mRNA levels, except for the three nonsense mutations very close to the end of the GFP coding sequence (PTC185ivs, PTC210ivs, and PTC231ivs) (Figure 2B). Also, there were no significant changes in mRNA levels between Region 1 and Region 2 (Figure 2C). In the presence of splicing, only mutations in the last 3rd of the coding region do not result in mRNA reduction. We examined whether the observed reductions are linked to *UPF1*. In the absence of *UPF1*, we observe a recovery of mRNA levels in Region 1 (PTC40ivs). But unexpectedly, we see an increase in PTC141ivs mRNA levels above the GFPivs-PTC-less mRNA (Figure 2D). We confirmed that our qPCR primers were specific for the spliced transcripts and that we didn't detect any corresponding pre-mRNA unspliced bands (Supplementary Figure 1D). We then questioned whether these changes are due to alterations in RNA stability. Although we didn't test the stability of PTC141ivs compared to WT-GFP, the splicing of the intron-containing reporters does not appear to affect the mRNA stability of the transcripts (Figure 2E). We observed an increase in mRNA levels in the GFPivs reporter compared to mRNAs from the intronless GFP reporter (Figure 2F). Since the increased mRNA levels do not correlate with increase in mRNA stability (as seen in Figure 2E), we investigated what other mechanisms may be involved. We found that despite the reporters having the same promoter, that there's more Pol II loading with GFPivs reporter (Figure 2G), suggesting that transcripts produced from intron-containing genes are transcribed more efficiently than those without introns.

Previously, we showed that knocking out *RNPS1* or *MAGO* did not affect splicing-dependent NMD (11). We then tested if *knocking out* Y14 impacts this process (Supplementary Figure 2A). We couldn't test using a *Δfal1* strain because we had issues growing it. As a control, we used the *Δmago* strain containing the WT-GFPivs, PTC40ivs, and PTC141ivs plasmids. As in the Δ*mago* strain, we did not obtain any rescue with *Δy14* (supplementary Figures 2A and B). Overall, our data show that splicing alters the effects of nonsense mutations on mRNA levels; that NMD depends on the PTC's proximity to the intron, and that the EJC is not involved in splicing-dependent NMD in *S. pombe*.

Discussion

In this study, we performed detailed mutagenesis experiments using GFP reporter constructs, both with and without introns, to understand how nonsense mutations within the GFP ORF affect RNA levels in fission yeast, *S. pombe*. While our results indicate that nonsense mutations lead to an observed reduction in mRNA levels when present at the beginning of the gene, consistent with early studies in *Saccharomyces cerevisiae* (16), which is in line with the 3' UTR NMD model, we found an increase in mRNA levels upon *UPF1* ablation compared to wild-type. Some nonsense mutations in Region 2 show higher mRNA levels above the PTCless GFP, and upon *UPF1* ablation, we observe a further increase in mRNA levels. This is completely in disagreement with the notion of an mRNA surveillance mechanism (15). In the intronless GFP reporter, all early PTCs tested were subject to NMD, including at codon 1. This finding contrasts with results from mammalian systems, where NMD has been studied extensively. In these systems, interactions between the translation termination machinery and the poly(A)-binding protein (PABPC1), or translation re-initiation at a downstream ATG start codon, typically suppress NMD (8, 17, 18). However, a study by Li and co-workers (19) using TCR-ß receptors also showed a 2-fold decrease in transcript levels when the first ATG codon was mutated, although the underlying mechanism was unknown. Mutating the ATG start codon is supposed to block NMD, as there would be no initiator codon for the ribosome to begin translation, since NMD is believed to be translation-coupled. However, PTC1 can still cause NMD if an upstream alternative ATG codon is present. Counting from the transcription start site of the *nmt41* promoter up to the first ATG codon of GFP, we did not detect any alternate ATG codon. The alternative explanation would be that translation might initiate at a near-cognate non-ATG codon or at an out-of-frame ATG codon (20-22). Since translation at these sites is inefficient, the transcripts are likely targeted for degradation.

A previous study using deletion and mutational analysis reported that the minimal domain necessary for GFP fluorescence lies between codons 7-229 (23). Therefore, codon position 231 falls outside this minimal domain and is not required for GFP expression or fluorescence. However, PTC231 led to increased mRNA levels. Together with previous studies showing that the resulting truncated protein remains functional, this finding challenges the assumption that cells universally degrade mRNAs containing premature termination codons. It is unclear why a PTC would lead to higher transcript levels than a WT transcript. PTCs 141 and 185 in GFP fall within the minimal domain necessary for GFP expression (23), which should prevent GFP expression. Yet, transcripts with these mutations were more abundant than the WT-GFP transcript. While it is difficult to speculate how these mutations cause an increase in transcript levels without a corresponding rise in GFP expression, it's possible that these mutations influence other RNA-processing steps (24).

For the late PTCs, our data showed that the increased mRNA abundance obtained with these transcripts isn't due to increased stability. Using PTC 141 as a proof of concept, we demonstrated that the mRNA produced by the reporter had stability similar to that of WT-GFP. The NMD-permissive PTC-containing transcripts are, in part, subject to NMD because they are significantly less stable. Therefore, these transcripts are more prone to degradation than non-PTC-containing transcripts since deletion of the core NMD factor *UPF1* abrogated NMD. The deletion of *UPF1* ultimately rescued the PTC6 NMD phenotype to WT levels and partially stabilized the transcripts. Since PTC-containing transcripts can be targets for either exonucleolytic or endonucleolytic decay pathways (25, 26), future experiments will evaluate how the poly(A) tail is processed in these mutants. While it is expected that the transcripts' poly(A) tails would be shorter due to deadenylation (27, 28), our previous study in *Drosophila* showed that PTC-containing transcripts actually have longer poly(A) tails (24). Additionally, short poly(A)tails have been found to be conserved among highly expressed genes (29).

As previously described (11), we also observed that splicing changes the effects that nonsense mutations have on mRNA levels. We found that, in the presence of splicing, most of the nonsense mutations result in a reduction in mRNA levels throughout the coding region except for the last three PTCs. Specifically, splicing abolished NMD sensitivity between the previously classified NMD-sensitive (Region 1, PTC1–88) and NMD-insensitive regions (Region 2, PTC108–231), extending our previous findings (11). However, we noted that there's more mRNA in the spliced constructs than in the unspliced constructs. This is not because we increase stability; instead, it is likely driven by an unidentified mechanism that we are unaware of. Splicing does not appear to affect the stability of the constructs we have examined. In fact, the changes in mRNA levels in the spliced construct may be an underestimate, as this transcript appears to be spliced at a higher level. Whereas previously (11), only *mago* and *rnps1* were tested, here we have also shown that *y14* isn't involved in *S. pombe* NMD. The non-involvement of the EJC in NMD is also observed in several other eukaryotes (30-32).

In summary, contrary to the notion that cells have a mechanism that detects PTC-containing mRNAs as aberrant transcripts and destroys them by a specialised mechanism, we found that nonsense mutations can also increase mRNA levels without altering their stability, implying that nonsense mutations can increase mRNA production through some yet unknown mechanisms. Somehow, a nonsense mutation fortuitously led to increased mRNA production. While splicing improved transcription and eliminated NMD sensitivity, as seen with an intron, mRNA decay depended on the distance of the PTC from the intron. Both the nonsense mutation-dependent mRNA reduction and increase observed in our study are inconsistent with the idea that cells have a mechanism to detect premature translation termination events specifically for eliminating certain mRNAs.

Materials and Methods

Yeast strains

The list of *S. pombe* strains used in this study is shown in Supplementary Table 1.

Plasmid construction and integration

The plasmids used in this study were derived from the pDUAL vector (33). All plasmid manipulations were performed on the pDUAL-GFP plasmid (11). The different PTC mutations at codon positions 1, 40, 53, 88, 108, 112, 126, 161, 185, 210, and 231 were introduced into the pDUAL-GFP plasmid using site-directed mutagenesis (34, 35) with some modifications. We used the Q5 DNA polymerase enzyme (New England Biolabs), along with primer pairs that have non-overlapping sequences at their 3' end and complementary, overlapping sequences at the 5' end. The PTC mutations were placed in the overlapping complementary sequences. We chose a minimum of 6 bases upstream and downstream of the desired codon mutations to correspond to the primer's complementary (overlapping) regions, with the primers terminating in a guanine or a cytosine. Our mutagenesis primers were about 50-60 bases in length, and the minimum melting temperature (T_m) difference between the non-overlapping and overlapping regions was 3°C. The non-overlapping regions were designed to be longer and of higher T_m than the overlapping regions. Using these parameters, a two-stage PCR protocol was performed in a single run for each mutation. The first stage involved a standard PCR cycle: initial denaturation at 98°C for 30 seconds (1 cycle), followed by 30-40 cycles of denaturation at 98°C for 10 seconds, annealing at a temperature dependent on the non-overlapping sequence for 30 seconds, extension at 72°C for 30 seconds per kilobase of plasmid, and a final extension at 72°C for 10 minutes. The second stage included an optional denaturation at 98°C for 10 seconds, followed by 1-3 cycles of annealing at a temperature dependent on the overlapping sequence, and a final extension at 72°C for 10 minutes. All mutations were confirmed by Sanger sequencing. The amplified plasmids were then treated with DpnI to destroy the methylated template plasmid before integration. To generate the intron-containing versions of the plasmids, the pDUAL-GFP plasmids with the nonsense mutations were digested with Pml1 restriction endonuclease, and the second intron of *ubc4* was amplified from *S. pombe* genomic DNA and cloned into the cut site at codon 110 using the NEBuilder HiFi DNA assembly kit (New England Biolabs) following the manufacturer's instructions. To generate the NMD reporter strains, the plasmids were integrated into the *leu1* locus as previously described (11, 33) in the WT, *Δupf1, Δmago, Δy14,* and the Flag-Rpb3 tagged strains. The list of primers used in this study is shown in Supplementary Table 2.

RNA extraction, analysis, and RNA stability quantification

Total RNA was extracted using the hot acid-phenol method (36). After extraction, the total RNA was treated with DNase I (1 unit) (Thermo Scientific) according to the manufacturer's instructions. First-strand cDNA synthesis was performed with the FastGene Scriptase II cDNA synthesis kit (Nippon Genetics) using 50 ng of total RNA, according to the manufacturer's instructions. Quantitative real-time PCR assays were conducted in 96-well plates using the ABI Prism™ SDS 7000 real-time PCR thermocycler (Applied Biosystems), following the manufacturer's instructions. PCR assays were performed using the qPCRBIO SyGreen Blue Mix Hi-ROX (PCR Biosystems). The $2^{-\Delta\Delta CT}$ method was used to calculate the relative expression levels of the target transcripts, normalised to *rpl32* mRNA or 18S rRNA. To inhibit transcription, cells were cultured to OD_{600} (~0.7) in PMG media and treated with 300 µg/mL 1,10-phenanthroline (Sigma). At different time points (0, 5, 10, 20, 40, and 60 minutes) immediately after adding the drug, 10 mL aliquots were transferred into 50 mL Falcon tubes containing about one volume of crushed ice before RNA extraction.

Chromatin immunoprecipitation (ChIP)

Freshly harvested cells from exponentially growing cultures (OD_{600} = 0.5) were fixed for 5 minutes at room temperature with 1% formaldehyde (Sigma Aldrich), followed by 10 minutes incubation with a further addition of glycine to stop the cross-linking. ChIP was then conducted as previously described (37).

Microscopy, and image quantification

Freshly harvested cells from exponentially growing cultures (OD600 = 0.5) were used. 1 mL of the culture was briefly centrifuged to pellet the cells. The supernatant was discarded, and the pellet was washed in 1 mL of sterile H_2O. After a brief second centrifugation to pellet the cells, the supernatant was discarded again, and the pellet was resuspended in sterile water. A 5 µL aliquot of the cell suspension was transferred to a slide with a coverslip, prepared for viewing under the Nikon Eclipse Ti fluorescence microscope. DIC images were captured with an exposure time of 100 ms, while GFP fluorescence (FITC) was visualized with an exposure time of 5 s using immersion oil objectives. Image quantification was performed with ImageJ, and total cell fluorescence was calculated using the formula CTCF = Integrated Density – (Area of the selected cell × Mean background fluorescence).

Statistical analysis

Statistical analysis was performed using GraphPad Prism™, which was also utilized to generate the figures. A t-test was employed to compare significant differences between the control and experimental groups when the data were normally distributed. When the data were not normally distributed, the Mann-Whitney Rank Sum test was used. For more than two data groups, ANOVA statistics were followed by Dunnett's multiple comparisons. Statistical significance is indicated with absolute P values.

Acknowledgement

The Authors acknowledge funding from the Biological Sciences Research Council [BB/M022757/1], The Darwin Trust of Edinburgh (to POO), and Bangabandhu Science and Technology Fellowship Trust (to MNH).

Figures and associated supplementary figures with legends

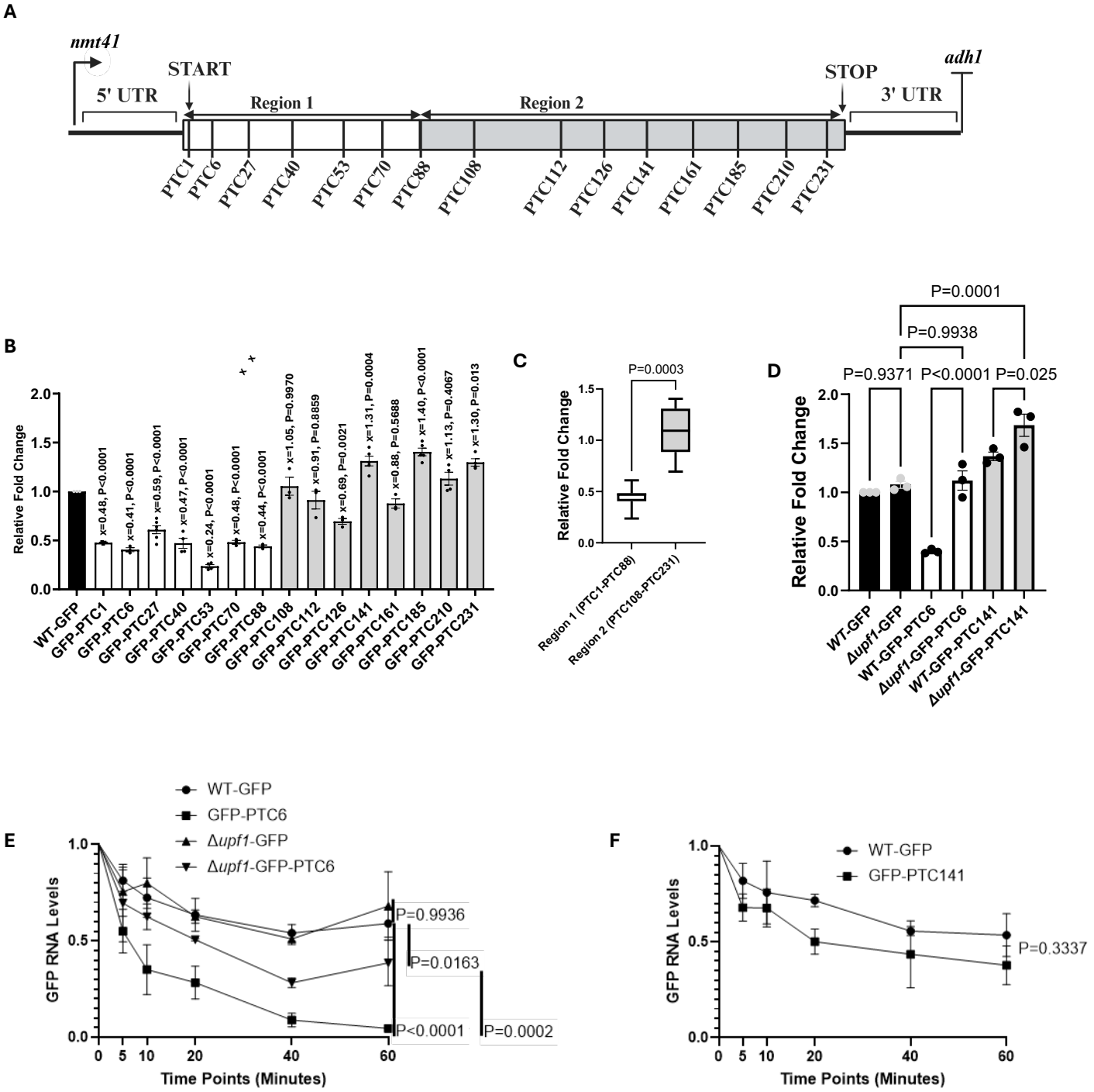
A
nmt41
START
5' UTR
Region 1
Region 2
STOP
3' UTR
adh1
PTC1
PTC6
PTC27
PTC40
PTC53
PTC70
PTC88
PTC108
PTC112
PTC126
PTC141
PTC161
PTC185
PTC210
PTC231
B
Relative Fold Change
x=0.48, P<0.0001
x=0.41, P<0.0001
x=0.59, P<0.0001
x=0.47, P<0.0001
x=0.24, P<0.0001
x=0.48, P<0.0001
x=0.44, P<0.0001
x=1.05, P=0.9970
x=0.91, P=0.8859
x=0.69, P=0.0021
x=1.31, P=0.0004
x=0.88, P=0.5688
x=1.40, P<0.0001
x=1.13, P=0.4067
x=1.30, P=0.013
WT-GFP
GFP-PTC1
GFP-PTC6
GFP-PTC27
GFP-PTC40
GFP-PTC53
GFP-PTC70
GFP-PTC88
GFP-PTC108
GFP-PTC112
GFP-PTC126
GFP-PTC141
GFP-PTC161
GFP-PTC185
GFP-PTC210
GFP-PTC231
C
P=0.0003
Relative Fold Change
Region 1 (PTC1-PTC88)
Region 2 (PTC108-PTC231)
D
P=0.0001
P=0.9938
P=0.9371
P<0.0001
P=0.025
Relative Fold Change
WT-GFP
Δupf1-GFP
WT-GFP-PTC6
Δupf1-GFP-PTC6
WT-GFP-PTC141
Δupf1-GFP-PTC141
E
WT-GFP
GFP-PTC6
Δupf1-GFP
Δupf1-GFP-PTC6
GFP RNA Levels
P=0.9936
P=0.0163
P<0.0001
P=0.0002
Time Points (Minutes)
F
WT-GFP
GFP-PTC141
GFP RNA Levels
P=0.3337
Time Points (Minutes)

Figure 1: Nonsense mutations can increase as well as reduce mRNA levels. A) Schematic of the pDUAL-GFP construct with the nonsense mutation positions. The codon sequence is split into two regions: Region 1, where mutations reduce mRNA levels, and Region 2, where mutations either increase or do not change mRNA levels. Image was created using Biorender. **B)** qRT-PCR comparing transcript levels of the GFP-PTC-containing transcripts. All data were normalised to WT-GFP RNA levels, with Rpl32 serving as an internal control. Error bars indicate standard errors from replicate experiments (at least three biological replicates were used in all cases, as represented by the data points). A one-way ANOVA with Dunnett's multiple comparisons was used to test for statistical significance (**x̄**= mean fold change value). **C)** Cumulative comparison of the mean fold-change values of mutations in Region 1 (PTC1-88) and mutations in Region 2 (PTC108-231). Mann-Whitney rank sum test was used to test for statistical significance. **D)** qRT-PCR comparing transcript levels of WT GFP, *Δupf1*-GFP, GFP-PTC6, *Δupf1*-GFP-PTC6, GFP-PTC141, and *Δupf1*-GFP-PTC141. Transcript levels were normalised to Rpl32, as an internal control. Error bars represent the standard error of the mean values between replicate experiments (n=3). A one-way ANOVA with Dunnett's multiple comparisons was used to test for statistical significance. **E)** RNA stability quantifications of the WT-GFP, GFP-PTC6, *Δupf1*-GFP, and *Δupf1*-PTC6 transcripts after treatment with 1,10 phenanthroline (300 µg/mL) for the indicated time points. At least three independent biological replicates were used for each experiment. 18S rRNA was used as the internal control for qRT-PCR. For each transcript, each time point was normalised to time 0 (T0) in that transcript. Error bars represent the standard error of the mean between replicate experiments. A 2-way ANOVA with Dunnett's multiple comparisons was used to test for statistical significance. **F)** RNA stability quantifications of the WT-GFP and GFP-PTC141 as in **E**. Error bars represent the standard error of the mean between replicate experiments (n=3). A t-test was used to test for statistical significance.

Supplementary Figure 1

A

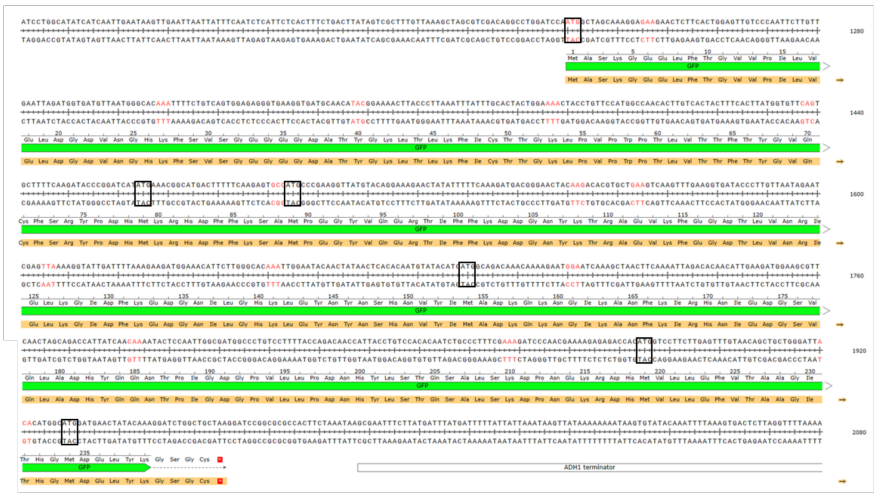

B

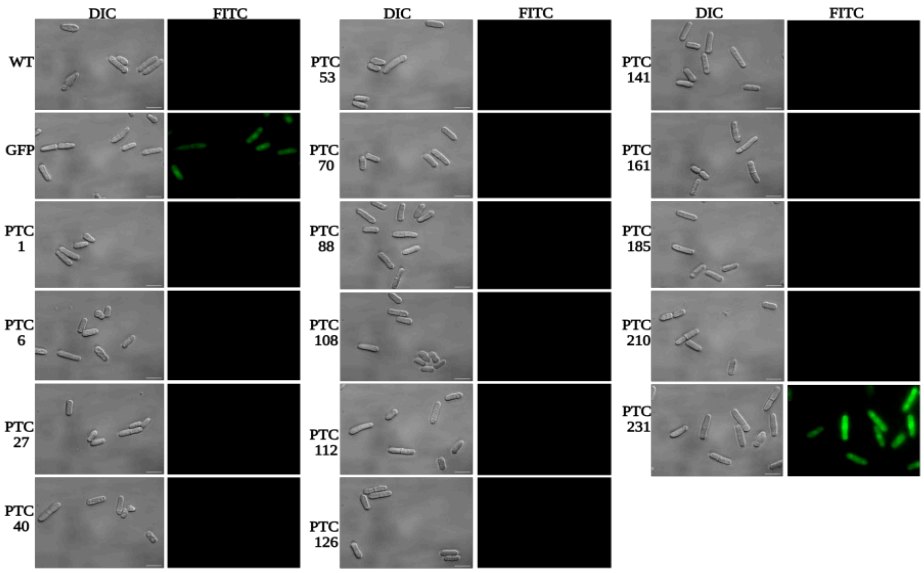

C

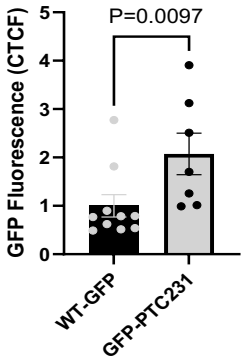

D

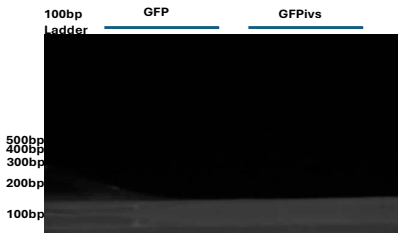

Supplementary Figure 1: Characterisation of reporters. A) GFP coding sequence. Nonsense codon positions are noted in red. The codons in each case were changed to a PTC using site-directed mutagenesis. The sequences highlighted in the outer-filled black boxes indicate ATG codons within GFP. The image was taken using SnapGene viewer. **B)** Representative DIC and fluorescence (FITC) images of the WT, GFP, and GFP-PTC-containing strains. Scale bars = 10µm. **C)** Image quantification of the GFP and GFP-PTC231 cells from **B**. 10 WT-GFP and 7 GFP-PTC231 independent cultures were imaged, and the corresponding images were quantified using ImageJ to compare GFP fluorescence. The mean fluorescence values are shown. Error bars represent the standard error of the mean across replicates. In each image, four individual cells were quantified, totalling 40 cells for WT-GFP and 28 for GFP-PTC231. Mann-Whitney rank sum test was used to test for statistical significance. **D)** Validation of the NMD qRT-PCR primers. PCR was performed under saturating conditions (40 cycles) to increase the chance of detecting any pre-mRNA or unspliced transcripts using three independent WT-GFP and WT-GFPivs cDNAs, and to verify that the qRT-PCR primers (GFP-qPCR-F and GFP-qPCR-R, sequences in Supplementary Table 2) were specific for the spliced transcript (in this case, GFP). Both primer pairs are compatible with GFP and GFPivs, since during splicing the intron is removed, producing only spliced GFP with a cDNA similar to that of WT-GFP. A 1% agarose gel was used.

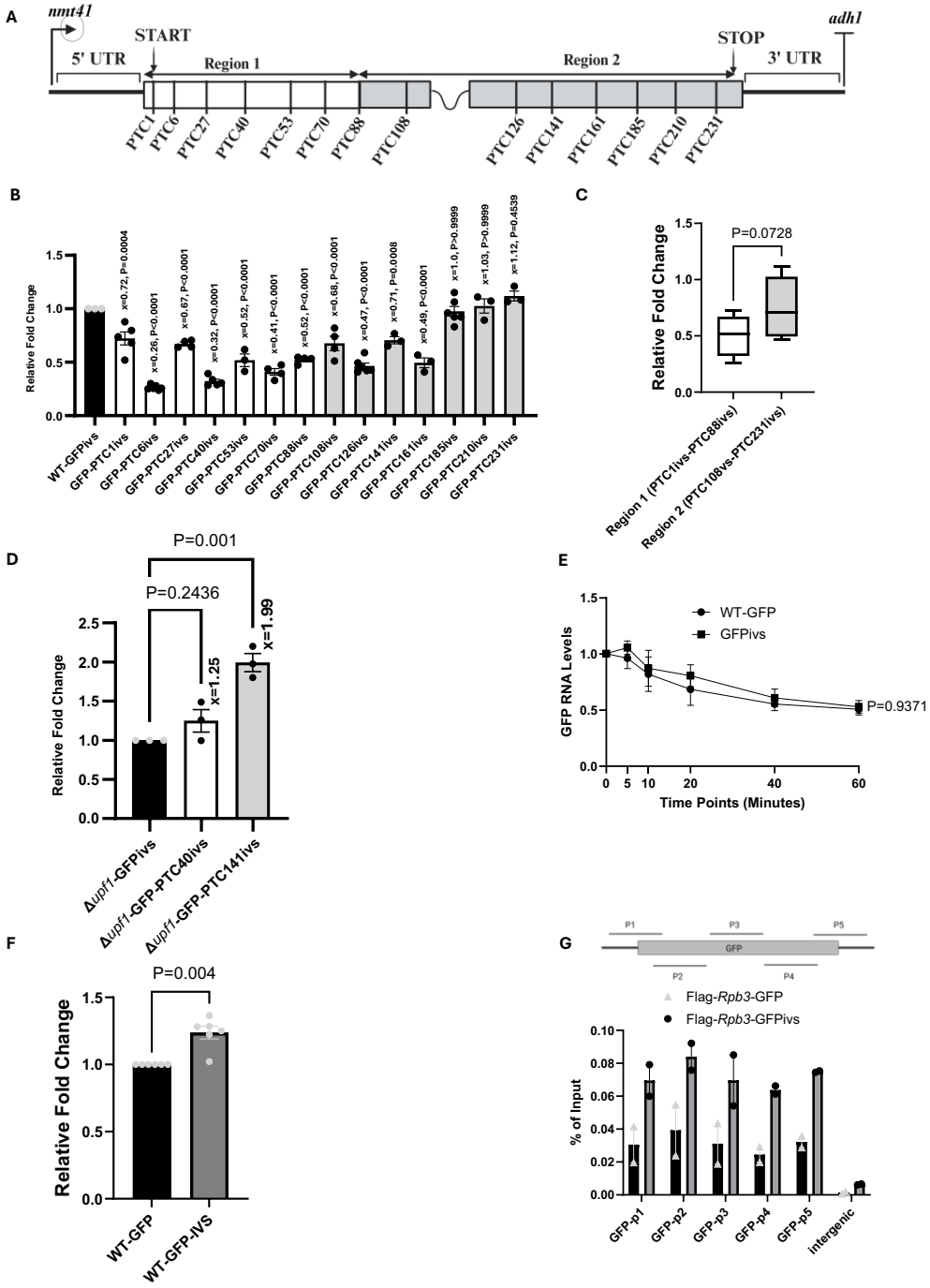
A
nmt41
START
5' UTR
Region 1
Region 2
STOP
3' UTR
adh1
PTC1
PTC6
PTC27
PTC40
PTC53
PTC70
PTC88
PTC108
PTC126
PTC141
PTC161
PTC185
PTC210
PTC231
B
Relative Fold Change
WT-GFPivs
GFP-PTC1ivs
GFP-PTC6ivs
GFP-PTC27ivs
GFP-PTC40ivs
GFP-PTC53ivs
GFP-PTC70ivs
GFP-PTC88ivs
GFP-PTC108ivs
GFP-PTC126ivs
GFP-PTC141ivs
GFP-PTC161ivs
GFP-PTC185ivs
GFP-PTC210ivs
GFP-PTC231ivs
C
P=0.0728
Relative Fold Change
Region 1 (PTC1ivs-PTC88ivs)
Region 2 (PTC108vs-PTC231ivs)
D
P=0.001
P=0.2436
x=1.25
x=1.99
Relative Fold Change
Δupf1-GFPivs
Δupf1-GFP-PTC40ivs
Δupf1-GFP-PTC141ivs
E
WT-GFP
GFPivs
GFP RNA Levels
P=0.9371
Time Points (Minutes)
F
P=0.004
Relative Fold Change
WT-GFP
WT-GFP-IVS
G
P1
P3
P5
GFP
P2
P4
Flag-Rpb3-GFP
Flag-Rpb3-GFPivs
% of Input
GFP-p1
GFP-p2
GFP-p3
GFP-p4
GFP-p5
intergenic

Figure 2

Figure 2: Splcing alters the effect of a nonsense mutation on mRNA levels. A) Schematic of the intron-containing versions of the pDUAL-GFP constructs (pDUAL-GFPivs) with the nonsense mutation positions. The codon sequence is split into two regions: Region 1, where mutations reduce mRNA levels, and Region 2, where mutations either increase or do not change mRNA levels. **B)** qRT-PCR comparing transcript levels of the GFP-PTCivs-containing transcripts. All data were normalised to WT-GFPivs RNA levels, with Rpl32 serving as an internal control. Error bars indicate standard errors from replicate experiments (at least three biological replicates were used in all cases, as represented by the data points). A one-way ANOVA with Dunnett's multiple comparisons was used to test for statistical significance **x̄**= mean fold change value). **C)** Cumulative comparison of the mean fold-change values of mutations in Region 1 (PTC1ivs-88ivs) and mutations in Region 2 (PTC108ivs-231ivs). Mann-Whitney rank sum test was used to test for statistical significance. **D)** qRT-PCR comparing transcript levels of *Δupf1*-GFPivs, *Δupf1*-GFP-PTC40ivs, and *Δupf1*-GFP-PTC141ivs. Transcript levels were normalised to *Δupf1*-GFPivs, with Rpl32 serving as an internal control. Error bars represent the standard error of the mean values between replicate experiments (n=3). A one-way ANOVA with Dunnett's multiple comparisons was used to test for statistical significance (**x̄**= mean fold change value)**. E)** RNA stability quantifications of the WT-GFP and WT-GFPivs after treatment with 1,10 phenanthroline (300 µg/mL) for the indicated time points. 18S rRNA was used as the internal control for qRT-PCR. For each transcript, each time point was normalized to time 0 (T0) in that transcript. Error bars represent the standard error of the mean between replicate experiments (n=5). A t-test was used to test for statistical significance. **F)** qRT-PCR comparing transcript levels of WT-GFP and WT-GFPivs. Transcript levels were normalised to WT-GFP, with Rpl32 serving as an internal control. Error bars represent the standard error of the mean values between replicate experiments (n=6). A t-test was used to test for statistical significance. **G)** ChIP-qPCR ChIP signal of Pol II ChIP signal (Flag-Rpb3) on WT-GFP and WT-GFPivs (n=2). The schematic above the bar chart shows the approximate positions of the ChIP qPCR primers on the GFP ORF. The primer sequences are listed in Supplementary Table 2.

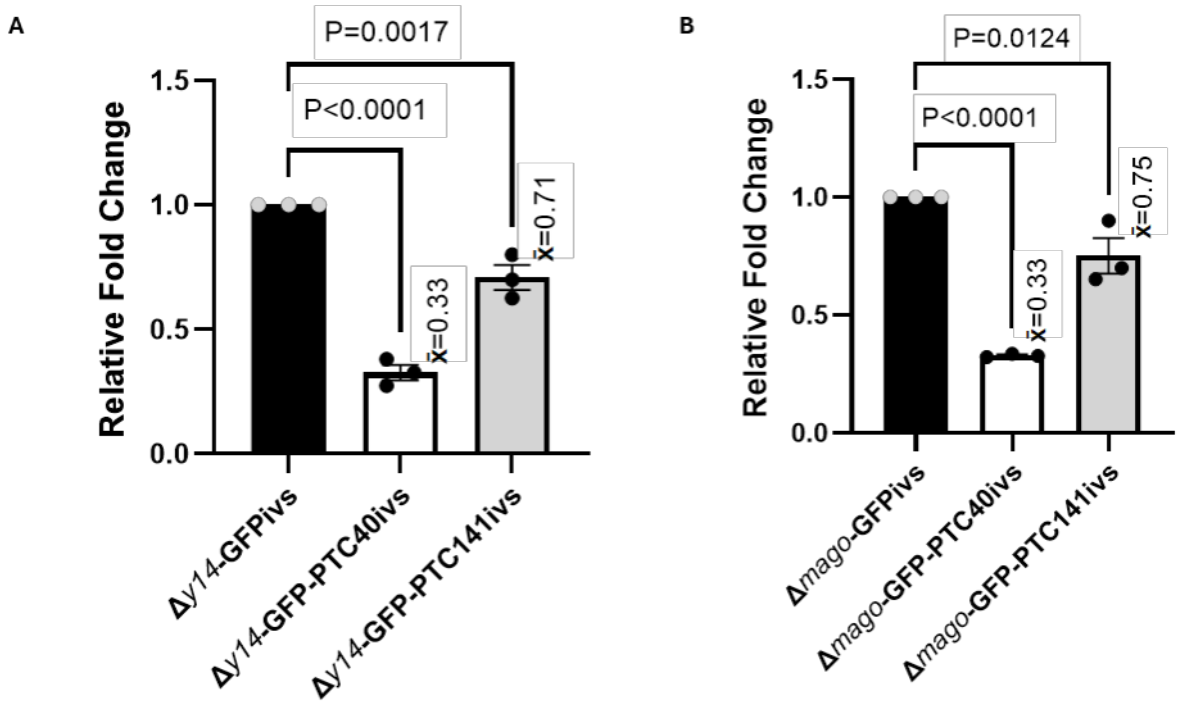

Supplementary Figure 2

Supplementary Figure 2: Splicing-dependent NMD does not require Y14 and MAGO in *Schizosaccharomyces pombe*. A) qRT-PCR comparing transcript levels of *Δy14*-GFPivs, *Δy14*-GFP-PTC40ivs, and *Δy14*-GFP-PTC141ivs. Transcript levels were normalised to *Δy14*-GFPivs, with *rpl32* serving as an internal control. Error bars represent the standard error of the mean values between replicate experiments (n=3). A one-way ANOVA with Dunnett's multiple comparisons was used to test for statistical significance (Significantly different comparisons = $P \leq 0.01$ to $P \leq 0.0001$, **x̄**= mean fold change value)**. B)** qRT-PCR comparing transcript levels of *Δmago*-GFPivs, *Δmago*-GFP-PTC40ivs, and *Δmago*-GFP-PTC141ivs. Transcript levels were normalised to *Δmago*-GFPivs, with Rpl32 serving as an internal control. Error bars represent the standard error of the mean values between replicate experiments (n=3). A one-way ANOVA with Dunnett's multiple comparisons was used to test for statistical significance (**x̄**= mean fold change value)

References

1. Brogna S, Wen J. Nonsense-mediated mRNA decay (NMD) mechanisms. Nat Struct Mol Biol. 2009;16(2):107-13.
2. Karousis ED, Muhlemann O. Nonsense-Mediated mRNA Decay Begins Where Translation Ends. Cold Spring Harb Perspect Biol. 2018.
3. Tan K, Wilkinson MF. Biological roles of nonsense-mediated RNA decay: insights from the nervous system. Curr Opin Genet Dev. 2025;93:102356.
4. Kurosaki T, Popp MW, Maquat LE. Quality and quantity control of gene expression by nonsense-mediated mRNA decay. Nat Rev Mol Cell Biol. 2019;20(7):406-20.
5. Le Hir H, Izaurralde E, Maquat LE, Moore MJ. The spliceosome deposits multiple proteins 20-24 nucleotides upstream of mRNA exon-exon junctions. EMBO J. 2000;19(24):6860-9.
6. Le Hir H, Gatfield D, Izaurralde E, Moore MJ. The exon-exon junction complex provides a binding platform for factors involved in mRNA export and nonsense-mediated mRNA decay. EMBO J. 2001;20(17):4987-97.
7. Shepard S, McCreary M, Fedorov A. The peculiarities of large intron splicing in animals. PLoS One. 2009;4(11):e7853.
8. Lindeboom RG, Supek F, Lehner B. The rules and impact of nonsense-mediated mRNA decay in human cancers. Nat Genet. 2016;48(10):1112-8.
9. Maquat LE, Li X. Mammalian heat shock p70 and histone H4 transcripts, which derive from naturally intronless genes, are immune to nonsense-mediated decay. Rna. 2001;7(3):445-56.
10. Brocke KS, Neu-Yilik G, Gehring NH, Hentze MW, Kulozik AE. The human intronless melanocortin 4-receptor gene is NMD insensitive. Hum Mol Genet. 2002;11(3):331-5.
11. Wen J, Brogna S. Splicing-dependent NMD does not require the EJC in Schizosaccharomyces pombe. EMBO J. 2010;29:1537-51.
12. Mendell JT, Medghalchi SM, Lake RG, Noensie EN, Dietz HC. Novel Upf2p orthologues suggest a functional link between translation initiation and nonsense surveillance complexes. Mol Cell Biol. 2000;20(23):8944-57.
13. Le Hir H, Andersen GR. Structural insights into the exon junction complex. Curr Opin Struct Biol. 2008;18(1):112-9.
14. Losson R, Lacroute F. Interference of nonsense mutations with eukaryotic messenger RNA stability. Proc Natl Acad Sci U S A. 1979;76(10):5134-7.
15. Brogna S, McLeod T, Petric M. The Meaning of NMD: Translate or Perish. Trends in Genetics. 2016;32(7):395-407.
16. Amrani N, Ganesan R, Kervestin S, Mangus DA, Ghosh S, Jacobson A. A faux 3'-UTR promotes aberrant termination and triggers nonsense-mediated mRNA decay. Nature. 2004;432:112-8.
17. Zhang J, Maquat LE. Evidence that translation reinitiation abrogates nonsense-mediated mRNA decay in mammalian cells. EMBO J. 1997;16(4):826-33.
18. Silva AL, Ribeiro P, Inacio A, Liebhaber SA, Romao L. Proximity of the poly(A)-binding protein to a premature termination codon inhibits mammalian nonsense-mediated mRNA decay. Rna. 2008;14(3):563-76.
19. Li S, Leonard D, Wilkinson MF. T cell receptor (TCR) mini-gene mRNA expression regulated by nonsense codons: a nuclear-associated translation-like mechanism. J Exp Med. 1997;185(6):985-92.
20. Brar GA, Yassour M, Friedman N, Regev A, Ingolia NT, Weissman JS. High-resolution view of the yeast meiotic program revealed by ribosome profiling. Science. 2012;335(6068):552-7.
21. Eisenberg AR, Higdon AL, Hollerer I, Fields AP, Jungreis I, Diamond PD, et al. Translation Initiation Site Profiling Reveals Widespread Synthesis of Non-AUG-Initiated Protein Isoforms in Yeast. Cell Syst. 2020.

22. Arribere JA, Gilbert WV. Roles for transcript leaders in translation and mRNA decay revealed by transcript leader sequencing. Genome Res. 2013;23(6):977-87.
23. Li X, Zhang G, Ngo N, Zhao X, Kain SR, Huang CC. Deletions of the Aequorea victoria green fluorescent protein define the minimal domain required for fluorescence. J Biol Chem. 1997;272(45):28545-9.
24. Brogna S. Nonsense mutations in the alcohol dehydrogenase gene of Drosophila melanogaster correlate with an abnormal 3' end processing of the corresponding pre-mRNA. Rna. 1999;5(4):562-73.
25. Schweingruber C, Rufener SC, Zund D, Yamashita A, Muhlemann O. Nonsense-mediated mRNA decay - mechanisms of substrate mRNA recognition and degradation in mammalian cells. Biochim Biophys Acta. 2013;1829(6-7):612-23.
26. Isken O, Maquat LE. Quality control of eukaryotic mRNA: safeguarding cells from abnormal mRNA function. Genes Dev. 2007;21(15):1833-56.
27. Parker R. RNA degradation in Saccharomyces cerevisae. Genetics. 2012;191(3):671-702.
28. Roy B, Jacobson A. The intimate relationships of mRNA decay and translation. Trends Genet. 2013;29(12):691-9.
29. Lima SA, Chipman LB, Nicholson AL, Chen YH, Yee BA, Yeo GW, et al. Short poly(A) tails are a conserved feature of highly expressed genes. Nat Struct Mol Biol. 2017;24(12):1057-63.
30. Longman D, Plasterk RH, Johnstone IL, Caceres JF. Mechanistic insights and identification of two novel factors in the C. elegans NMD pathway. Genes Dev. 2007;21(9):1075-85.
31. Gatfield D, Unterholzner L, Ciccarelli FD, Bork P, Izaurralde E. Nonsense-mediated mRNA decay in Drosophila: at the intersection of the yeast and mammalian pathways. EMBO J. 2003;22:3960–70.
32. Gabiatti BP, Freire ER, Odenwald J, de Freitas Nascimento J, Holetz F, Carrington M, et al. Trypanosomes lack a canonical EJC but possess an UPF1 dependent NMD-like pathway. PLoS One. 2025;20(3):e0315659.
33. Matsuyama A, Shirai A, Yashiroda Y, Kamata A, Horinouchi S, Yoshida M. pDUAL, a multipurpose, multicopy vector capable of chromosomal integration in fission yeast. Yeast. 2004;21(15):1289-305.
34. Liu H, Naismith JH. An efficient one-step site-directed deletion, insertion, single and multiple-site plasmid mutagenesis protocol. BMC Biotechnol. 2008;8:91.
35. Zheng L, Baumann U, Reymond JL. An efficient one-step site-directed and site-saturation mutagenesis protocol. Nucleic Acids Res. 2004;32(14):e115.
36. Collart MA, Oliviero S. Preparation of yeast RNA. Curr Protoc Mol Biol. 2001;Chapter 13:Unit13 2.
37. De S, Edwards DM, Dwivedi V, Wang J, Varsally W, Dixon HL, et al. Genome-wide chromosomal association of Upf1 is linked to Pol II transcription in Schizosaccharomyces pombe. Nucleic Acids Res. 2022;50(1):350-67.

Supplementary Table 1: Yeast strains used in this study

Strain	Genotype	Source
WT-pDUAL-GFP	h+ *leu1*-32 *ura4*DS/E pDUAL-GFP	(11)
WT-pDUAL-GFP PTC1	h+ *leu1*-32 *ura4*DS/E pDUAL-GFP-PTC1	This study
WT-pDUAL-GFP-PTC6	h+ *leu1*-32 *ura4*DS/E pDUAL-GFP-PTC6	(11)
WT-pDUAL-GFP-PTC27	h+ *leu1*-32 *ura4*DS/E pDUAL-GFP-PTC27	(11)
WT-pDUAL-GFP-PTC40	h+ *leu1*-32 *ura4*DS/E pDUAL-GFP-PTC40	This study
WT-pDUAL-GFP-PTC53	h+ *leu1*-32 *ura4*DS/E pDUAL-GFP-PTC53	This study
WT-pDUAL-GFP-PTC70	h+ *leu1*-32 *ura4*DS/E pDUAL-GFP-PTC70	This study
WT-pDUAL-GFP-PTC108	h+ *leu1*-32 *ura4*DS/E pDUAL-GFP-PTC108	This study
WT-pDUAL-GFP-PTC112	h+ *leu1*-32 *ura4*DS/E pDUAL-GFP-PTC112	This study
WT-pDUAL GFP-PTC126	h+ *leu1*-32 *ura4*DS/E pDUAL-GFP-PTC126	This study
WT-pDUAL-GFP-PTC141	h+ *leu1*-32 *ura4*DS/E pDUAL-GFP-PTC141	This study
WT-pDUAL-GFP-PTC161	h+ *leu1*-32 *ura4*DS/E pDUAL-GFP-PTC161	This study
WT-pDUAL-GFP-PTC185	h+ *leu1*-32 *ura4*DS/E pDUAL-GFP-PTC185	This study
WT-pDUAL-GFP-PTC210	h+ *leu1*-32 *ura4*DS/E pDUAL-GFP-PTC210	This study
WT-pDUAL-GFP-PTC231	h+ *leu1*-32 *ura4*DS/E pDUAL-GFP-PTC231	This study
WT-pDUAL-GFPivs	h+ *leu1*-32 *ura4*DS/E pDUAL-GFPivs	This study
WT-pDUAL-GFP-PTC1ivs	h+ *leu1*-32 *ura4*DS/E pDUAL-GFP-PTC1ivs	This study
WT-pDUAL-GFP-PTC6ivs	h+ *leu1*-32 *ura4*DS/E pDUAL-GFP-PTC6ivs	This study
WT-pDUAL-GFP-PTC27ivs	h+ *leu1*-32 *ura4*DS/E pDUAL-GFP-PTC27ivs	This study
WT-pDUAL-GFP-PTC40ivs	h+ *leu1*-32 *ura4*DS/E pDUAL-GFP-PTC40ivs	This study
WT-pDUAL-GFP-PTC53ivs	h+ *leu1*-32 *ura4*DS/E pDUAL-GFP-PTC53ivs	This study
WT-pDUAL-GFP-PTC70ivs	h+ *leu1*-32 *ura4*DS/E pDUAL-GFP-PTC70ivs	This study
WT-pDUAL-GFP-PTC88ivs	h+ *leu1*-32 *ura4*DS/E pDUAL-GFP-PTC88ivs	This study
WT-pDUAL-GFP-PTC108ivs	h+ *leu1*-32 *ura4*DS/E pDUAL-GFP-PTC108ivs	This study
WT-pDUAL-GFP-PTC126ivs	h+ *leu1*-32 *ura4*DS/E pDUAL-GFP-PTC126ivs	This study
WT-pDUAL-GFP-PTC141ivs	h+ *leu1*-32 *ura4*DS/E pDUAL-GFP-PTC141ivs	This study
WT-pDUAL-GFP-PTC161ivs	h+ *leu1*-32 *ura4*DS/E pDUAL-GFP-PTC161ivs	This study
WT-pDUAL-GFP-PTC185ivs	h+ *leu1*-32 *ura4*DS/E pDUAL-GFP-PTC185ivs	This study
WT-pDUAL-GFP -PTC210ivs	h+ *leu1*-32 *ura4*DS/E pDUAL-GFP-PTC210ivs	This study
WT-pDUAL-GFP-PTC231ivs	h+ *leu1*-32 *ura4*DS/E pDUAL-GFP-PTC231ivs	This study
Δ*upf1*-pDUAL-GFP	h+ *ade6*-210 *arg3*D *his3*D *leu1*-32 *ura4*DS/E *upf1*:kanMX6 pDUAL-GFP	This study
Δ*upf1*-pDUAL-GFP-PTC6	h+ *ade6*-210 *arg3*D *his3*D *leu1*-32 *ura4*DS/E *upf1*:kanMX6 pDUAL-GFP-PTC6	This study
Δ*upf1*-pDUAL-GFP-PTC141	h+ *ade6*-210 *arg3*D *his3*D *leu1*-32 *ura4*DS/E *upf1*:kanMX6 pDUAL-GFP-PTC141	This study
Δ*upf1*-pDUAL-GFP-PTC40ivs	h+ *ade6*-210 *arg3*D *his3*D *leu1*-32 *ura4*DS/E *upf1*:kanMX6 pDUAL-GFP-PTC40ivs	This study
Δ*upf1*-pDUAL-GFP-PTC141ivs	h+ *ade6*-210 *arg3*D *his3*D *leu1*-32 *ura4*DS/E *upf1*:kanMX6 pDUAL-GFP-PTC141ivs	This study
Δ*mago*-pDUAL-GFPivs	h- *leu1*-32 *ura*D4-D18, *mago*del:clonatR pDUAL-GFPivs	This study
Δ*mago*-pDUAL-GFP-PTC40ivs	h- *leu1*-32 *ura*D4-D18, *mago*del:clonatR pDUAL-GFP-PTC40ivs	This study
Δ*mago*-pDUAL-GFP-PTC141ivs	h- *leu1*-32 *ura*D4-D18, *mago*del:clonatR pDUAL-GFP-PTC141ivs	This study

Δ*y14*-pDUAL-GFPivs	h- *leu1*-32 *ura*D4-D18, *y14*del:clonatR pDUAL-GFPivs	This study
Δ*y14*-pDUAL-GFP-PTC40ivs	h- *leu1*-32 *ura*D4-D18, *y14*del:clonatR pDUAL-GFP-PTC40ivs	This study
Δ*y14*-pDUAL-GFP-PTC141ivs	h- *leu1*-32 *ura*D4-D18, *y14*del:clonatR pDUAL-GFP-PTC141ivs	This study
Flag-Rpb3-WT-pDUAL-GFP	h- *leu1*-flag-rpb3 *ade*6-M216 *ura* D18 pDUAL-GFP	This study
Flag-Rpb3-WT-pDUAL-GFPivs	h- *leu1*-flag-rpb3 *ade*6-M216 *ura* D18 pDUAL-GFPivs	This study

Supplementary Table 2: Primers used in this study

Primer name	Description	Sequence
Ubc4_F	Ubc4 cloning	CAAAGATGACGGGAACTACAAGACACGTATGTAACTATTTAGTCTTGTGTAGATTATG
Ubc4_R	Ubc4 cloning	GTATCACCTTCAAACTTGACTTCAGCACCTACGAATATGCTGTTAGTTATC
GFP-qPCR-F	qPCR	GAGTTGTCCCAATTCTTGTT
GFP-qPCR-R	qPCR	CTTGACTTCAGCACGTGTCTT
PTC1 F	PTC1 mutagenesis	GGATCCATAGGCTAGCAAAGGAGAAGAACTCTTCACTGGAGTTGTCCCAATTCTTG
PTC1 R	PTC1 mutagenesis	GCTAGCCTATGGATCCAGGCCTGTCGACGCTAGCTTTAACAAAGCGACTATAAGTC
PTC40_F	PTC40 mutagenesis	GATGCAACATAAGGAAAACTTACCCTTAAATTTATTTGCACTACTGGAAAACTACCTG
PTC40_R	PTC40 mutagenesis	GTTTTCCTTATGTTGCATCACCTTCACCCTCTCCACTGACAGAAAATTTG
PTC53_F	PTC53 mutagenesis	CTACTGGATAACTACCTGTTCCATGGCCAACACTTGTCACTACTTTCAC
PTC53_R	PTC53 mutagenesis	CAGGTAGTTATCCAGTAGTGCAAATAAATTTAAGGGTAAGTTTTCCGTATGTTGCATC
PTC70_F	PTC70 mutagenesis	CTTATGGTGTTTAGTGCTTTTCAAGATACCCGGATCATATGAAACGGCATGAC
PTC70_R	PTC70 mutagenesis	CTTGAAAAGCACTAAACACCATAAGTGAAAGTAGTGACAAGTGTTGGCCATGGAAC
PTC88_F	PTC88 mutagenesis	CAAGAGTTAAATGCCCGAAGGTTATGTACAGGAAAGAACTATATTTTTCAAAGATGAC
PTC88_R	PTC88 mutagenesis	TCGGGCATTTAACTCTTGAAAAAGTCATGCCGTTTCATATGATCCGGGTATC
PTC108_F	PTC108 mutagenesis	GAACTACTAGACACGTGCTGAAGTCAAGTTTGAAGGTGATACCCTTGTTAATAG
PTC108_R	PTC108 mutagenesis	ACGTGTCTAGTAGTTCCCGTCATCTTTGAAAAATATAGTTCTTTCCTGTACATAACCTTC
PTC_112_F	PTC112 mutagenesis	CACGTGCTTAAGTCAAGTTTGAAGGTGATACCCTTGTTAATAGAATCGAGTTAAAAG
PTC_112_R	PTC112 mutagenesis	CTTGACTTAAGCACGTGTCTTGTAGTTCCCGTCATCTTTGAAAAATATAGTTCTTTCCTG
PTC126_F	PTC126 mutagenesis	GTTAATAGAATCGAGTAAAAAGGTATTGATTTTAAAGAAGATGGAAACATTCTTGGGCAC
PTC126_R	PTC126 mutagenesis	CAATACCTTTTTACTCGATTATATTAACAAGGGTATCACCTTCAAACTTGACTTCAG
PTC_161_F	PTC161 mutagenesis	CAAAAGAATTGAATCAAAGCTAACTTCAAAATTAGACACAACATTGAAGATGGAAG
PTC_161_R	PTC161 mutagenesis	CTTTGATTCAATTCTTTTGTTTGTCTGCCATGATGTATACATTGTGTGAGTTATAGTTG
PTC_185_F	PTC185 mutagenesis	CATTATCAATAAAATACTCCAATTGGCGATGGCCCTGTCCTTTTACCAGAC
PTC_185_R	PTC_185 mutagenesis	CAATTGGAGTATTTTATTGATAATGGTCTGCTAGTTGAACGCTTCCATCTTCAATGTTG
PTC_210_F	PTC_210 mutagenesis	CTTTCGTAAGATCCCAACGAAAAGAGAGACCACATGGTCCTTCTTGAGTTTGTAACAGC

PTC_210_R	PTC_210 mutagenesis	GTTGGGATCTTACGAAAGGGCAGATTGTGTGG ACAGGTAATGGTTGTCTGGTAAAAGGAC
PTC_231_F	PTC_231 mutagenesis	TGGGATTTGACATGGCATGGATGAACTATACAA AGGATCTGGCTG
PTC_231_R	PTC_231 mutagenesis	TGCCATGTCAAATCCCAGCAGCTGTTACAAAC TCAAGAAGGACCATG
Rpl32_F	qPCR	TGGATTGAAGGCTTTCCTAGTC
Rpl32_R	qPCR	CAGAGACGTTACCAGCAATCT
PTC108 qPCR_R	qPCR	CTTGACTTCAGCACGTGTCTA
18S F	qPCR	CAATTGGAGGGCAAGTCTGG
18S R	qPCR	GTCGACCAGGCTCAAAGTTC
Intergenic_F	ChIP qPCR	GAA CGA ACC AGG ACG GCT AT
Intergenic_R	ChIP qPCR	TGC ATG GAG GGT TTC CAC TC
ChIP_GFP_(P1)_F	ChIP qPCR	ACGATTACTGGGGAGAGAAAACA
ChIP_GFP_(P1)_R	ChIP qPCR	GTGCCCATTAACATCACCATCT
ChIP_GFP_(P2)_F	ChIP qPCR	GAGTTGTCCCAATTCTTGTTGA
ChIP_GFP_(P2)_R	ChIP qPCR	AGTGAAAGTAGTGACAAGTGTT
ChIP_GFP_(P3)_F	ChIP qPCR	TGCTTTTCAAGATACCCGGATCA
ChIP_GFP_(P3)_R	ChIP qPCR	GCCCAAGAATGTTTCCATCTTCT
ChIP_GFP_(P4)_F	ChIP qPCR	TGTATACATCATGGCAGACAAA
ChIP_GFP_(P4)_R	ChIP qPCR	GGTCTCTCTTTTCGTTGGGATCT
ChIP_GFP_(P5)_F	ChIP qPCR	TCCCAACGAAAAGAGAGACCA
ChIP_GFP_(P5)_F	ChIP qPCR	AGCGACCTCATACTATACCTGA